Transactions of the Korean Nuclear Society Spring Meeting
Jeju, Korea, May 29-30, 2014

Single photon image from PET with insertable collimator for boron neutron capture therapy

Joo-Young Jung[a], Key Jo Hong[b], Tae Suk Suh[a*]
[a]*Dept. of Biomedical Engineering and Research Institute of Biomedical Engineering, College of Medicine, Catholic University of Korea, Seoul 505, South Korea*
[b]*Molecular Imaging Program at Stanford (MIPS), Department of Radiology, Stanford University, 300 Pasteur Drive, Stanford, CA 94305,USA*
[*]*Corresponding author: suhsanta@catholic.ac.kr*

1. Introduction

Boron neutron capture therapy (BNCT) is a radiation therapy technique for treating deep-seated brain tumors by irradiation with a thermal neutron in which boron-labelled low molecular weight compounds [1]. Before the BNCT is started, a patient should be inspected using a positron emission tomography (PET) scan for the identification of region of molecular interactions caused by annihilation in the tumor cells, using an isotope exclusive to PET. Once completed, a single photon emission computed tomography (SPECT) scan is conducted to investigate for the region of therapy using an isotope exclusive to SPECT.

In the case of an existing PET/SPECT combination system, at least two types of isotopes should be used for each scan with their purposes [2]. Recently, researchers examined the effects of PET/SPECT dual modality on animal imaging systems [3]. They reported that the PET/SPECT combination system was effective for simultaneous achievement of a single event and coincidence [4]. The aim of our proposed system (Fig.1) is to confirm the feasibility of extraction of two types of images from one PET module with an insertable collimator for brain tumor treatment during the BNCT.

2. Materials and Methods

2.1 Simulation configuration

The positrons were emitted from the injected compound which is located on the tumor cell. The positron emission tomographic image could be acquired using annihilation events between positrons and electrons from the boron uptake regions. In order to simulate this reaction, the positron sources were distributed at the boron uptake regions in the simulation space. In addition, there were the five boron uptake regions in the virtual phantom and the PET detector with the collimator for the SPECT image detector. The purpose of using a virtual brain phantom was to compare the PET image with the SPECT image using the collimator on the PET detector for the BNCT. The diameter and height of the water cylinder were 20 cm and 6 cm, respectively. The density of the boron uptake region was set at 2.08 g/cm^3 [5].

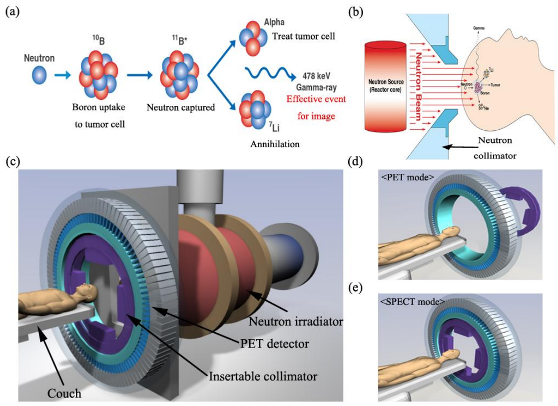

Fig. 1. (a) Physical mechanism of boron neutron capture therapy (BNCT), (b) neutron delivered to the uptake boron in brain tumor, (c) illustration of our proposed inserted collimator system for single photon emission computed tomography (SPECT) to acquire a single photon image on a positron emission tomography (PET) detector, (d) our proposed system for BNCT facility using only PET before treatment, (e) PET with insertable SPECT collimator during treatment.

2.2 PET detector module and image processing

The selection of the PET detector was significant for extracting effective events for image reconstruction. Although the PET image should be acquired from the detector, the reconstruction of the SPECT image using the insertable collimator on the PET detector should be considered. For these reasons, lutetium-yttrium oxyorthosilicate ($Lu_{0,6}$ $Y_{1,4}$ $Si_{0,5}$:Ce, LYSO) was chosen as the detector material for achieving satisfactory performance. LYSO has a relatively high density of 7.3 g/cm^3, which causes a high probability of photon deposition events [6]. The inner diameter and thickness of the detector were 80 cm and 3 cm, respectively. For reconstruction of the PET image, the existence of 511 keV annihilation events was investigated by spectrum analysis using the pulse height distribution tally (F8-tally) function in MCNPX. The annihilation events from the five boron uptake regions were collected from P-trac data, which was the MCNPX output data for particle tracking. The collected annihilation events were used to compose the PET sinogram, whose angle was 180°. The number of profile grid was set to 80. The decision of grid size was based on the minimum value to permit reconstruction of image without reduction of matrix size. This grid size was possible to reconstruct image using a few event numbers using applied matrix size and to reduce reconstruction time in this study. The PET image was reconstructed with this sinogram data using the ordered subset expectation maximization (OSEM) algorithm.

2.3 Insertable SPECT collimator and image processing

After the acquisition of PET images, the neutron source was emitted from outside the brain phantom. The distance between the source and the center of the phantom was 20 cm. The energy of the neutron source was set to the thermal neutron level (<1 eV). The energy level of the thermal neutron is used in actual BNCT. The 478 keV prompt gamma ray from the boron neutron capture reaction was emitted. The discrimination of prompt gamma ray peak was also performed by the verification of energy spectrum using the F8-tally function in MCNPX. The event of the prompt gamma ray was detected by the PET detector using the customized parallel collimator. The structure of the parallel collimator was remodeled from the original structure to adapt it to a ring detector. The projection data was collected by the rotation of phantom on a center axis. The SPECT sinogram was composed of 120 projections at 3° each. The reconstruction of the SPECT image progressed using the OSEM reconstruction algorithm similarly to the reconstruction of the PET image.

2.4 Image evaluations

First, the vertical and horizontal image profiles were collected from the reconstructed images for analysis of the full width at half maximum (FWHM) values of the five boron uptake regions. Second, to evaluate the accuracy of each reconstructed image, the receiver operating characteristic (ROC) curve of the five boron uptake regions was compiled. The ROC curve was quantitatively analyzed by calculating the area under the curve (AUC) from both the PET and the SPECT images.

3. Results and Discussion

Fig. 2 shows the spectra of the annihilation event and the prompt gamma ray. Fig. 2(a) is the spectrum including the annihilation event by the positron from the boron uptake regions. The gamma ray events at 511 keV were counted by the detector clearly on the spectrum, with a FWHM value of 41 keV (8.0%). After the neutron emission, the 478 keV prompt gamma ray events were also visible on the spectrum, with a FWHM value of 31 keV (6.4%), as shown in Fig. 2(b). Both the PET and SPECT images were reconstructed using the OSEM algorithm. Fig. 2(c) shows the original pattern of the virtual brain phantom including the five boron uptake regions. Based on these boron uptake regions, the Fig. 2(d) shows the reconstructed PET image using the annihilation events by the positrons. Fig. 2(e) shows the reconstructed SPECT image that was acquired using the insertable collimator. The size of boron uptake regions in the image was slightly larger than that in the PET image because the reaction rate of boron neutron capture is different from the reaction rate of annihilation events.

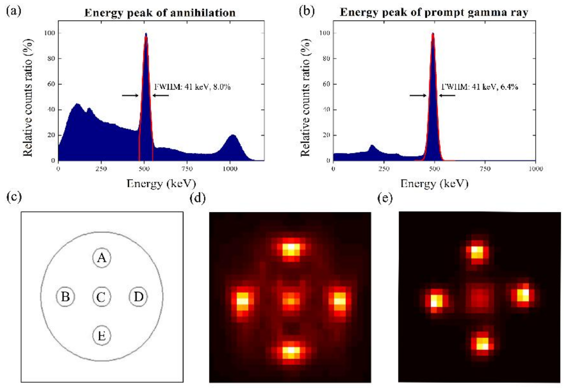

Fig. 2. Top: Spectral characteristics and full width at half maximum (FWHM) values on (a) energy peak of annihilation event using positron emission tomography (PET) module and (b) prompt gamma ray event from boron uptake regions using insertable single photon emission computed tomography (SPECT) collimator with PET module. Bottom: (c) Original pattern of brain phantom in the simulation; the boron uptake regions are represented as A to E surrounded by water material in this figure; (d) reconstructed PET image using ordered subset expectation maximization (OSEM) algorithm; and (e) reconstructed single photon image with insertable SPECT collimator on the PET module using OSEM algorithm.

As shown in Fig. 3, the simulation results are shown for four kinds of signal profiles. In order to analyze the reconstructed image quantitatively, the profiles in the horizontal and vertical planes were measured from both the PET and the insertable SPECT collimator images.

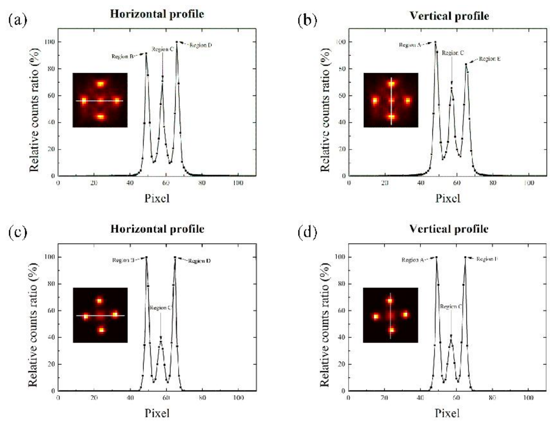

Fig. 3. Profiles of horizontal and vertical lines including the five uptake regions in the phantom. The top figures ((a) and (b)) are image profiles of the positron emission tomography (PET) image and the bottom, figures ((c) and (d)) are image profiles of the single photon emission computed tomography (SPECT) image.

Finally, to evaluate the accuracy of reconstructed image, the ROC curve analysis was performed. Figs. 4(a) and (b) respectively show the ROC curves based on the PET and SPECT images with the insertable collimator. The AUC values for the five boron uptake regions were calculated using the ROC curve data. The PET AUC values of five regions (Region A: 0.80, Region B: 0.78, Region C: 0.71, Region D: 0.78, and Region E: 0.80) were greater than 0.7. On the other hand, the SPECT AUC values of two regions (Region A: 0.90 and Region D: 0.90) were greater than 0.9, and the AUC values of Region B and Region E were calculated to be 0.89 and 0.89, respectively. The only AUC value of Region C was recorded as the 0.78. Fig. 4(b) shows that the ROC curve patterns of all regions were almost the same between the two images. As mentioned earlier, the accuracy of reconstruction of Region C was influenced by the geometric conditions and the number of projections. The AUC values for all five regions also show a similar tendency.

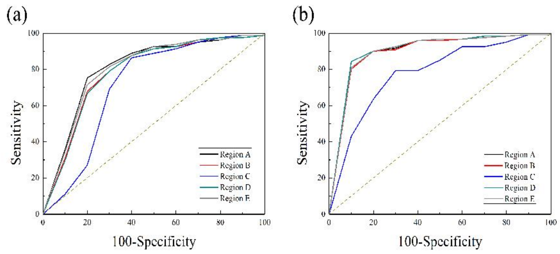

Fig. 4. Receiver operating characteristic (ROC) curve of (a) reconstructed image of positron emission tomography (PET) and (b) reconstructed image of single photon emission computed tomography (SPECT). The area under the curve (AUC) values of each region was calculated from the ROC curves.

In the further, the actual experiment based on this study will be conducted using an in-house insertable collimator. If the BNCT SPET system (PET/SPECT system) shows good performance, we can observe the region treated by radiation in real time. This study, as well as further research, is expected to be useful in constructing a radiation treatment planning system for BNCT.

4. Conclusions

We attempted to acquire the PET and SPECT images simultaneously using only PET without an additional isotope. Single photon images were acquired using an insertable collimator on a PET detector.

REFERENCES

[1] R.F. Barth, J.C. Grecula, W. Yang, J.H. Rotaru, M. Nawrocky, N. Gupta, B.J. Albertson, A.K. Ferketich, M.L. Moeschberger, J.A. Coderre, E.K. Rofstad, Combination of boron neutron capture therapy and external beam radiotherapy for brain tumors, International Journal of Radiation Oncology • Biology • Physics, Vol.58, p.267, 2004.

[2] A. Kjaer, Molecular imaging of cancer using PET and SPECT, in New trends in cancer for the 21st century Springer, p.277, 2006.

[3] A. Bartoli, N. Belcari, A. Del Guerra, S. Fabbri, Simultaneous PET/SPECT imaging with the small animal scanner YAP-(S) PET, IEEE Nuclear Science Symposium conference record, Vol.5, p.3408, 2007.

[4] Yao, R, Beaudoin, J. F, Deng, X, Cadorette, J, Lecomte, R, Imaging performance of a PET/SPECT dual modality animal system, IEEE Nuclear Science Symposium conference record p.2418, 2011.

[5] D. K. Yoon, J.Y. Jung, K. J. Hong, T. S. Suh, Tomographic image of prompt gamma ray from boron neutron capture therapy: A Monte Carlo simulation study, Applied Physics Letters, Vol.104, 083521, 2014.

[6] K.J. Hong, Y. Choi, J.H. Jung, J. Kang, W. Hu, H.K. Lim, Y. Huh, S. Kim, J.W. Jung, K.B. Kim, A prototype MR insertable brain PET using tileable GAPD arrays, Medical Physics, Vol.40, 042503, 2013.